ONE IN A HUNDRED MILLION

New Developments in Direct Contrast Ratio Imaging with a Charge-Injection Device

Sailee Sawant

Ph.D. Advisor: Dr. Daniel Batcheldor

Department of Aerospace, Physics and Space Sciences
Florida Institute of Technology

237th AAS Meeting Press Conference

Email: ssawant2011@my.fit.edu
Phone: +1 321-960-5268

January 15, 2021

Candle Next to the Lighthouse: Faint Target vs. Bright Source

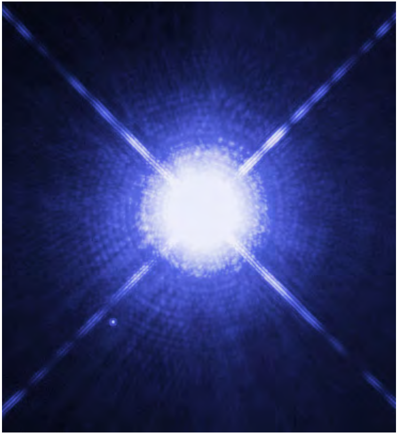

Figure 1: Sirius A (center) and its faint stellar companion, Sirius B (lower left). This $0.24' \times 0.26'$ image was taken on October 15, 2003 with Hubble's Wide Field Planetary Camera 2 [Bond et al., 2017]

- Charge-coupled Devices (CCDs)
- Complementary metal-oxide-semiconductor (CMOS) devices

Disadvantages:

- Limited full well capacity
- Charge saturation
- Limited dynamic range

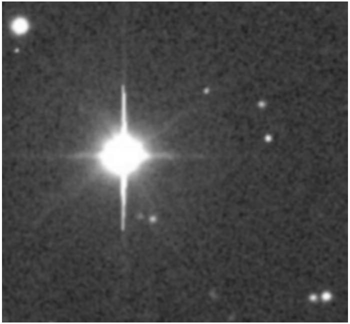

Figure 2: Charge saturation and blooming on a CCD image [Chromey, 2010]

$\Rightarrow$ **Directly achievable contrast ratios:** $\log_{10}(\mathrm{CR}) < 5$

Current Techniques

Objective: To suppress signals from bright sources
Method: Point-spread function (PSF) subtraction

- Coronography [Schneider et al., 2010]
- Ground-based Angular Differential Imaging [Marois et al., 2006]
- Spaced-based Roll Subtraction Imaging [Lowrance et al., 2005, Schneider et al., 2010]
- Nulling Interferometry [Bracewell and MacPhie, 1979, Linfield, 2003]

$\Rightarrow$ **Achievable contrast ratios:** $5 < \log_{10}(CR) < 7$

Operational Requirements:

- Similar target and template PSFs
- High wavefront quality
- Stable pointing and tracking controls
- Additional optical elements

$\Rightarrow$ **complex, expensive, and time-consuming**

An Important Question

How do we conduct observations for contrasts that are many more orders of magnitudes higher and for targets that are at even smaller angular separations?

Potential Solution:

Use charge-injection devices (CIDs) for direct extreme contrast ratio (ECR) imaging

Benefits:

- Simple
- Cost-Effective
- Practical

Some major advantages [Bhaskaran et al., 2008]:

- Adaptive dynamic range $\Rightarrow$ Theoretical $\log_{10}(\mathrm{CR}) \sim 9.6$, or $\Delta m \sim 24$
- Inherently anti-blooming
- Randomly addressable pixels
- Non-destructive readout (NDRO) capability

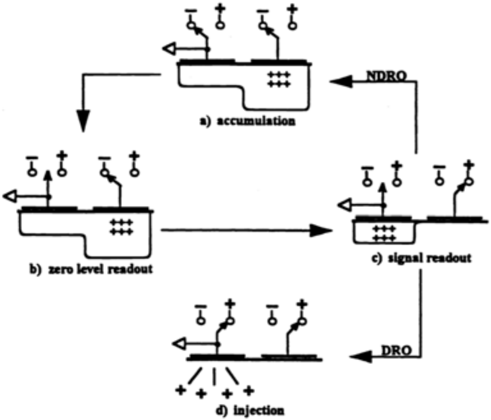

Figure 3: Basic CID readout operation [Ninkov et al., 1994]: (a) charge accumulation, (b) zero level readout, (c) Signal readout, (d) charge injection

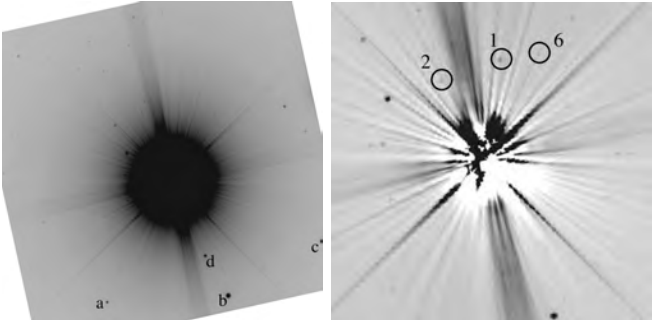

Figure 4: The (left) 13′ and (right) 3′.25 radius fields around Sirius [Batcheldor et al., 2016].

- Detector: SpectraCAM XDR (SXDR)
- Telescope: Florida Tech 0.8 m Ortega, Florida
- Filter: V-Band
- Exposure Time: 20 seconds

Object	m_v (mag)	Raw log(CR)
Sirius	-1.46	
1	14.2	6.3
2	14.5	6.4
6	16.8	7.3

Table 1: V-Band magnitudes [Bonnet-Bidaud and Gry, 1991].

Next Step: Sirius Field Observations from La Palma

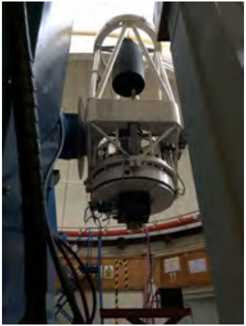

- **Telescope:** Jacobus Kapteyn Telescope (JKT)
- **Observation Site:** Roque de los Muchachos, La Palma, Canary Isles
- **Aperture Size:** 1.0 m

Sirius Field

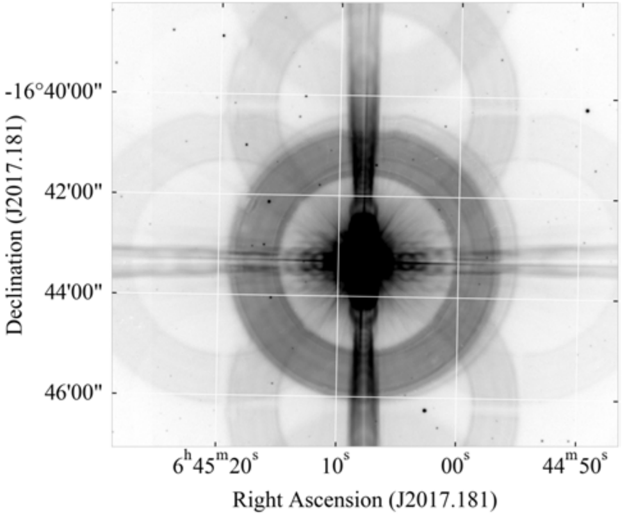

Figure 5: Pre-processed I-Band SXDR image of the Sirius Field with an exposure time of 180 seconds. The signal from Sirius is not saturated.

Results: 1 Part in 100 Million

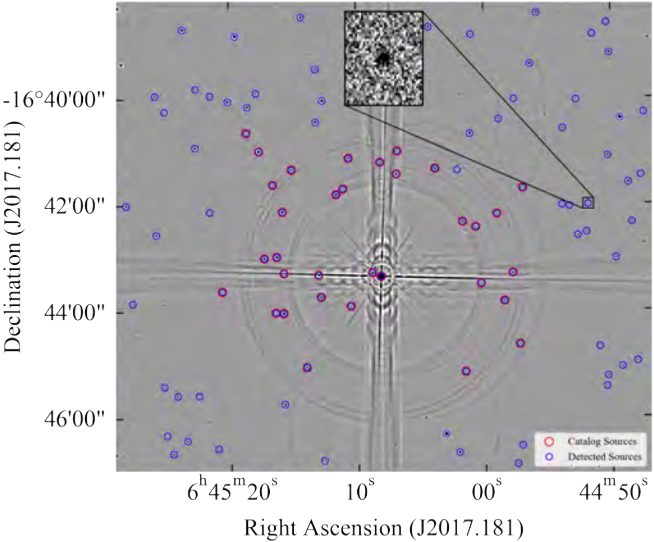

Figure 6: The SIMBAD catalog sources (red) and detected sources (blue) overlaid on the post-processed I-Band SXDR image of the Sirius Field

Results: 1 Part in 100 Million (cont.)

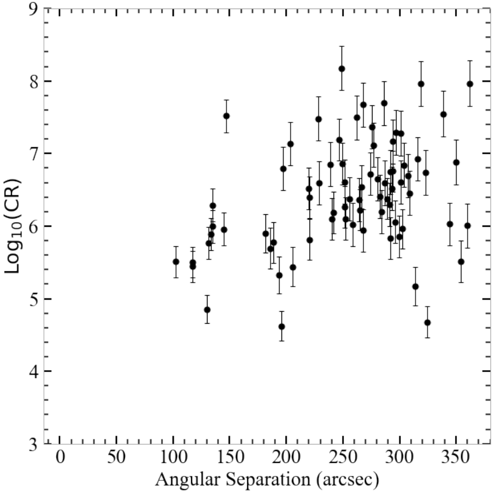

Figure 7: $\log_{10}(CR)$ as a function of angular separation in arcseconds for the I-Band SXDR image of the Sirius Field

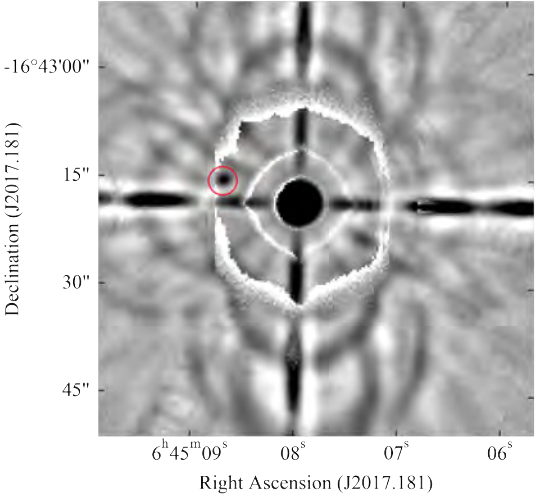

Figure 8: Sirius A (center), and its faint stellar companion, Sirius B (marked in red)

8 months CID Technology Demonstration [Batcheldor et al., 2020]

Figure 9: CID camera mounted to the Kibo Exposed Facility on-board the *International Space Station (ISS)*

⇒ **No significant on-orbit changes in terms of dark current, linearity, read noise, and photon transfer efficiency**
⇒ **CIDs are now space-qualified to Technology Readiness Level 8 (TRL-8) and can be considered for future space telescopes**

Summary

- Acquired unsaturated SXDR images of the Sirius field with an exposure time of 180 seconds.
- Detected and resolved previously uncatalogued sources, along with Sirius B, without imposing complex operational requirements.
- Demonstrated a direct achievable contrast ratio of 1:100 million with a 1.0 m telescope
- Delivered a simple, cost-effective, yet powerful technique that combines CID imaging and software-based image analysis
- Next step is to carry out CID imaging from an observing site with $\sim$ 2.5 m telescope (For example, 2.54 m Issac Newton Telescope, La Palma)
  - To detect even fainter sources
  - To achieve even higher contrast ratios

Contact Info: Email: ssawant2011@my.fit.edu **Phone:** +1 321-960-5268

D. Batcheldor, R. Foadi, C. Bahr, J. Jenne, Z. Ninkov, S. Bhaskaran, and T. Chapman. Extreme contrast ratio imaging of sirius with a charge injection device. *Publications of the Astronomical Society of the Pacific*, 128(960):025001, jan 2016. doi: 10.1088/1538-3873/128/960/025001.

D. Batcheldor, S. Sawant, J. Jenne, Z. Ninkov, S. Durrance, S. Bhaskaran, and T. Chapman. Charge Injection Device Performance in Low-Earth Orbit. , 132(1011):055001, May 2020. doi: 10.1088/1538-3873/ab7a74.

Suraj Bhaskaran, Tony Chapman, Michael Pilon, and S Vangorden. Performance based cid imaging–past, present and future. *Proceedings of SPIE - The International Society for Optical Engineering*, 7055, 08 2008. doi: 10.1117/12.795235.

Howard E. Bond, Gail H. Schaefer, Ronald L. Gilliland, Jay B. Holberg, Brian D. Mason, Irving W. Lindenblad, Miranda Seitz-McLeese, W. David Arnett, Pierre Demarque, Federico Spada, Patrick A. Young, Martin A. Barstow, Matthew R. Burleigh, and Donald Gudehus. The Sirius System and Its Astrophysical Puzzles: Hubble Space Telescope and Ground-based Astrometry. , 840(2):70, May 2017. doi: 10.3847/1538-4357/aa6af8.

J. M. Bonnet-Bidaud and C. Gry. The stellar field in the vicinity of Sirius and the color enigma. , 252:193, Dec 1991.

R. N. Bracewell and R. H. MacPhie. Searching for nonsolar planets. , 38(1):136–147, Apr 1979. doi: 10.1016/0019-1035(79)90093-9.

Frederick R. Chromey. *To Measure the Sky: An Introduction to Observational Astronomy*. Cambridge University Press, 2010. doi: 10.1017/CBO9780511794810.

References (cont.)

Roger P. Linfield. Technology requirements and development path for planet detection by mid-IR interferometry. In Michael Shao, editor, *Interferometry in Space*, volume 4852, pages 443 – 450. International Society for Optics and Photonics, SPIE, 2003. doi: 10.1117/12.460862. URL https://doi.org/10.1117/12.460862.

Patrick J. Lowrance, E. E. Becklin, Glenn Schneider, J. Davy Kirkpatrick, Alycia J. Weinberger, B. Zuckerman, Christophe Dumas, Jean-Luc Beuzit, Phil Plait, Eliot Malumuth, Sally Heap, Richard J. Terrile, and Dean C. Hines. An Infrared Coronagraphic Survey for Substellar Companions. , 130(4): 1845–1861, Oct 2005. doi: 10.1086/432839.

Christian Marois, David Lafrenière, René Doyon, Bruce Macintosh, and Daniel Nadeau. Angular Differential Imaging: A Powerful High-Contrast Imaging Technique. , 641(1):556–564, Apr 2006. doi: 10.1086/500401.

Zoran Ninkov, Chen Tang, Brian S. Backer, Roger L. Easton, and Joseph M. Carbone. Charge injection devices for use in astronomy. In *Astronomical Telescopes and Instrumentation*, 1994.

Glenn Schneider, Murray D. Silverstone, Elizabeth Stobie, Joseph H. Rhee, and Dean C. Hines. NICMOS Coronagraphy: Recalibration and the NICMOS Legacy Archive PSF Library. In *Hubble after SM4. Preparing JWST*, page 15, Jul 2010.

CCD vs. CID

	CCD	CID
Detector Name	Andor Ikon-L 936	SpectraCam XDR (SXDR)
Type	Back-Illuminated	Front-Illuminated
Operational Temperature	-99.0°C	-45.6°C
Physical Area (pixels $\times$ pixels)	2048 $\times$ 2048	2048 $\times$ 2048
Pixel Size (microns)	13.5 $\times$ 13.5	12.0 $\times$ 12.0
Pixel Scale	0.34″/pixel	0.30″/pixel.
Field of View	11′.6 $\times$ 11′.6	10′.0 $\times$ 10′.0
Gain (e^-/ADU)	1.0	6.2
QE (at 525 nm ($\sim$ V-band))	95%	48%
Full Well Capacity	100,000 e^-	Linear (within 2%) $\rightarrow$ 268,000 e^-, Saturation $\rightarrow$ 305,000 e^-
Read Noise	6.3 e^-	Single Read: 44 e^- RMS, 128 NDROs: 5.8 e^- RMS

Bright Stars:

Proper Name	Bayer Designation	Henry Draper (HD) Catalogue Name	RA (hh mm ss) (J2000.0)	DEC (dd mm ss) (J2000.0)	Spectral Type	V (mag)	B - V (mag)	V - R (mag)	R - I (mag)	V - I (mag)	Parallax (mas)
Aldebaran	* alf Tau	HD 29139	04 35 55.24	+16 30 33.49	K5	0.860	1.540	1.230	0.940	2.170	48.94
Alpheratz	* alf And	HD 358	00 08 23.26	+29 05 25.55	B8	2.060	-0.110	-0.030	-0.100	-0.130	33.62
Altair	* alf Aql	HD 187642	19 50 47.00	+08 52 05.96	A7	0.760	0.220	0.140	0.130	0.270	194.95
Arcturus	* alf Boo	HD 124897	14 15 39.67	+19 10 56.67	K1	-0.050	1.230	0.980	0.650	1.630	88.83
Betelgeuse	* alf Ori	HD 39801	05 55 10.31	+07 24 25.43	M1	0.420	1.850	1.590	1.280	2.870	6.55
Castor	* alf Gem	HD 60179	07 34 35.87	+31 53 17.82	A1	1.580	0.040	0.070	-0.010	0.060	64.12
Deneb	* alf Cyg	HD 197345	20 41 25.92	+45 16 49.22	A2	1.250	0.090	0.110	0.100	0.210	2.31
Pollux	* bet Gem	HD 62509	07 45 18.95	+28 01 34.32	K0	1.140	1.000	0.750	0.500	1.250	96.54
Procyon	* alf CMi	HD 61421	07 39 18.12	+05 13 29.96	F5	0.370	0.420	0.420	0.230	0.650	284.56
Scheat	* bet Peg	HD 217906	23 03 46.46	+28 04 58.03	M2	2.420	1.670	1.500	1.320	2.820	16.64
Sirius	* alf CMa	HD 48915	06 45 08.92	-16 42 58.02	A1	-1.460	0.000	0.000	-0.030	-0.030	379.21
Spica	* alf Vir	HD 116658	13 25 11.58	-11 09 40.75	B1	0.970	-0.230	-0.090	-0.240	-0.330	13.06
Vega	* alf Lyr	HD 172167	18 36 56.34	+38 47 01.28	A0	0.030	0.000	-0.040	-0.030	-0.070	130.23

Simulated Star Field